The *Sept4* Septin Locus Is Required for Sperm Terminal Differentiation in Mice

Holger Kissel,[1] Maria-Magdalena Georgescu,[1,5]
Sarit Larisch,[1,3] Katia Manova,[4] Gary R. Hunnicutt,[2]
and Hermann Steller[1,*]
[1]Howard Hughes Medical Institute and
The Rockefeller University
Laboratory of Apoptosis and Cancer Biology
1230 York Avenue
Box 252
New York, New York 10021
[2]Population Council
The Rockefeller University
1230 York Avenue
Box 273
New York, New York 10021
[3]Apoptosis and Cancer Research Laboratory
Pathology Department
Rambam Medical Center
Haifa 31096
Israel
[4]Developmental Biology Program
Molecular Cytology Core Facility
Memorial Sloan Kettering Cancer Center
1275 York Avenue
New York, New York 10021

Summary

The murine *septin4* gene (*Sept4*) has been implicated in diverse cellular functions, including cytokinesis, apoptosis, and tumor suppression. Here, we investigated the function of *Sept4* proteins during mouse development by creating a targeted deletion of the *Sept4* genomic locus. *Sept4* mutant mice are viable but male sterile due to immotile and structurally defective sperm. During spermatogenesis, *Sept4* proteins were essential for proper mitochondrial architecture and establishment of the annulus, a ring-like structure in the tail region of sperm. In addition, *Sept4* mutant sperm showed defects in the elimination of residual cytoplasm during sperm maturation and had increased staining for the caspase inhibitor XIAP. This is consistent with a role of the proapoptotic *Sept4* protein ARTS in promoting caspase-mediated removal of cytoplasm via inhibition of XIAP. Our results indicate that *Sept4* proteins play distinct but evolutionarily conserved functions in different cellular compartments.

Introduction

Septins comprise a family of proteins whose overall structure has been conserved from yeast to *Drosophila* to humans. Septins are GTPases related to the Ras su-

perfamily of signaling GTPases that are thought to mediate their function through formation of macromolecular, heterooligomeric filaments, often referred to as the septin cytoskeleton (Faty et al., 2002; Field et al., 2002; Kartmann and Roth, 2001). Septins were first described in the budding yeast *Saccharomyces cerevisiae* in a screen for mutations blocking cell cycle progression (Hartwell, 1971). Genetic studies in yeast and *Drosophila* together with biochemical analyses have provided a molecular concept of how these proteins regulate a variety of processes, including mitotic entry and cytokinesis (Faty et al., 2002). Correct assembly of septins at the mother/daughter bud neck and continued maintenance of the septin ring at the bud/cleavage site are essential for the completion of cytokinesis (Barral et al., 2000; Castillon et al., 2003). Two working models for septin biology have been described (Longtine and Bi, 2003). The "scaffold model" proposes that the septin cytoskeleton directs the assembly of signaling complexes, thereby linking cytoskeletal rearrangements with activation of the mitotic machinery (Moffat and Andrews, 2003). The "diffusion-barrier model" is based on the ability of the septin ring to generate cell polarity and maintain an asymmetric distribution of signaling proteins and membrane material between mother and daughter cell (Takizawa et al., 2000). These two working models are not mutually exclusive, and both proposed mechanisms may contribute to successful mitosis. Formation of the septin ring, as observed at the cleavage site during cytokinesis, appears to be a dynamic process that can change between linear and ring-like states depending on cellular physiology (Dobbelaere et al., 2003; Kinoshita et al., 2002).

In mammalian cells, Septin2/Nedd5, Septin9/MSF, and, indirectly, Septin4/H5 have been implicated in the completion of cytokinesis (Kim et al., 2004; Surka et al., 2002; Zhang et al., 1999). In addition, a variety of cellular functions, including vesicle trafficking and cytoskeletal filament formation, have been attributed to septins in postmitotic cells, especially in the central nervous system (Kartmann and Roth, 2001). Furthermore, a proapoptotic septin termed ARTS (apoptosis-related protein in the TGF-β signaling pathway) has been identified as one of four splice variants derived from the *Sept4* locus (Larisch et al., 2000; Larisch-Bloch et al., 2000). ARTS localizes to mitochondria in living cells and has been proposed to play an important and general role in the induction of apoptosis through a variety of stimuli (Larisch et al., 2000). ARTS promotes apoptosis, at least in part, by potentiating caspase activity via antagonizing Inhibitor of Apoptosis proteins (IAPs), such as XIAP (Gottfried et al., 2004). IAPs comprise a family of important negative regulators of apoptosis that can directly inhibit active caspases, the key executioners of apoptosis (reviewed in Salvesen and Abrams, 2004). Furthermore, ARTS appears to be a tumor suppressor in acute lymphoblastic leukemia (ALL): ARTS, but not the *Sept4*/H5, protein was specifically lost with high frequency in ALL patients, and loss of ARTS correlated with the disease state (Elhasid et al., 2004).

*Correspondence: steller@mail.rockefeller.edu
[5]Present address: Department of Neuro-Oncology & Molecular Genetics, The University of Texas M.D. Anderson Cancer Center, Houston, Texas 77030.

To investigate the function of *Sept4* proteins in vivo, we generated a *Sept4* deletion in the mouse germline, thereby eliminating all transcripts generated at this locus. Homozygous mutant mice were viable and displayed no overt aberrations compared to wild-type (wt) mice. However, mutant males were sterile due to an essential requirement of *Sept4* proteins during the post-meiotic stages of spermatogenesis, known as spermiogenesis. Mutant sperm had several distinct structural defects, including defective mitochondrial architecture, bent and nonmotile tails, absence of the annulus, and defects in the removal of residual cytoplasm. Taken together with previous work demonstrating a proapoptotic activity of ARTS (Gottfried et al., 2004; Larisch et al., 2000), our results reveal a surprisingly complex role of this locus in both the formation of filamentous structures and the regulation of caspase activity during sperm maturation.

Results

Targeting of the Murine *Sept4* Locus

Analogous to the human *Sept4* gene, three different open reading frames have been previously described for *Sept4* in the mouse, including Sept4/H5, Sept4/Cdcrel-2b, and Sept4/M-Septin (Figure 1A). In addition, we identified the mouse homolog of the human proapoptotic variant Sept4/hARTS, by using its unique C terminus to search an EST database (Figure 1A). Just like its human homolog, *Sept4*/mARTS (GenBank accession CF553913) uses an upstream transcriptional initiation site, exon 1a, but lacks exon 2 of full-length *SEPT4*/H5 found in the human ARTS protein (Figure 1A). Both proteins are highly homologous, differing mostly in the length of the unique C terminus (Figure S1A; see the Supplemental Data available with this article online), which is generated through a new in-frame stop codon from intron 6 as a consequence of alternative splicing (Figure 1A) (Larisch et al., 2000). Figure 1B summarizes and compares the features of the different murine *Sept4* proteins. Northern blot analysis of mouse tissues by using a probe spanning exons 3–6, common to all isoforms, showed the highest *Sept4* expression in brain and testis and, to a lesser extent, in heart, lung, and kidney (Figure 1C). Rehybridization of the filter with a probe specific to the unique C terminus of mARTS confirmed the expression of ARTS mRNA in testis (Figure 1C), with its level of expression ranging from 20%–40% of the full-length septins, depending on tissue type (Figure 1C, lower panel). In addition, RT-PCR on testis and brain RNA with a primer specific for the unique C terminus of mARTS also confirmed the presence of a transcript encoding the ARTS protein isoform in both tissues (Figure S1B). The large size of the testis transcripts appears to be due to tissue-specific splicing and the presence of unique 5′ and 3′ UTRs in testis, consistent with the unique regulation of transcription in spermatogenesis (Sassone-Corsi, 2002). Finally, we used a *Sept4*-GFP reporter mouse strain to investigate the temporal regulation of *Sept4* transcription during spermiogenesis (Figure 2, see below).

To investigate the function of *Sept4* proteins in the mouse, we used a standard gene targeting strategy. To generate a complete loss-of-function mutant, we eliminated virtually the entire *Sept4* genomic locus (Figure 1D). Successful targeting was confirmed by Southern blot analysis of PstI-digested genomic tail DNA, showing the presence of the diagnostic 3.9 kb genomic fragment (Figure 1E, left panel). To confirm the absence of different *Sept4* proteins in homozygous mutant mice, we probed protein extracts derived from the cerebellum with an antibody raised against a peptide from exon 1 (generous gift from S. Yanagi) (Takahashi et al., 2003) and confirmed the absence of *Sept4* isoforms H5 and M-Septin in homozygous mutant mice by Western blot analysis (Figure 1E, right panel).

Sept4 Null Males Display Male Sterility

Sept4 null mice were born at Mendelian frequencies (F2 wt = 38, het = 85, null = 37) and showed no obvious phenotypic abnormalities. However, *Sept4* had a nonredundant and essential function in the testis that is necessary for male fertility. Mating of eight *Sept4* null males with different females over a period of 5–8 months yielded no offspring. No *Sept4* null male was ever observed to sire offspring, even though the presence of seminal plugs in female mice confirmed normal copulation. Testis and epididymis of mutant males appeared normal, with no significant difference in testicular weight (wt 91 ± 9 mg, N = 6; null 110 ± 7 mg, N = 7) and no difference in cauda epididymal sperm numbers (data not shown). Histological examination of mutant testis showed no overt effect of the mutation at any stage of germ cell development (Figures 2A and 2B), and tubules of wt and homozygous mutant epididymides were filled with sperm (Figures 2C and 2D). Furthermore, no decline in testicular morphology was observed in ageing *Sept4* null males. To determine the expression profile of *Sept4* proteins, we utilized a BAC (bacterial artificial chromosome) transgenic mouse line in which the endogenous protein coding sequence has been replaced by an EGFP reporter gene (Gong et al., 2003). RNA in situ hybridization with a GFP-specific probe revealed *Sept4* promoter activity strictly confined to stage V–VII tubules (Figure 2E, Figure S2). The signal was specifically localized to postmeiotic stages, and transcripts accumulated in round spermatids, indicating that *Sept4* is specifically expressed during postmeiotic differentiation and the process of spermiogenesis.

Lack of Motility and Structural Defects in *Sept4* Mutant Sperm

Microscopic examination of sperm removed from the cauda epididymis of *Sept4*-deficient males revealed a complete lack of motility by these gametes (Movies 1 and 2). In addition, about 50%–70% of mutant sperm displayed a severe bending of the tail region, typically at 180°, suggesting a structural defect caused by the *Sept4* mutation. To stage the onset of these abnormal phenotypes, we isolated spermatozoa from the testis as well as the three regions of the epididymis (caput, corpus, cauda). As shown in Figure 3, wt sperm showed occasional modest bending in the caput epididymis, usually associated with the location of the cytoplasmic droplet (asterisk, Figure 3A). Further passage through the epididymis resulted in the typical linear morphology
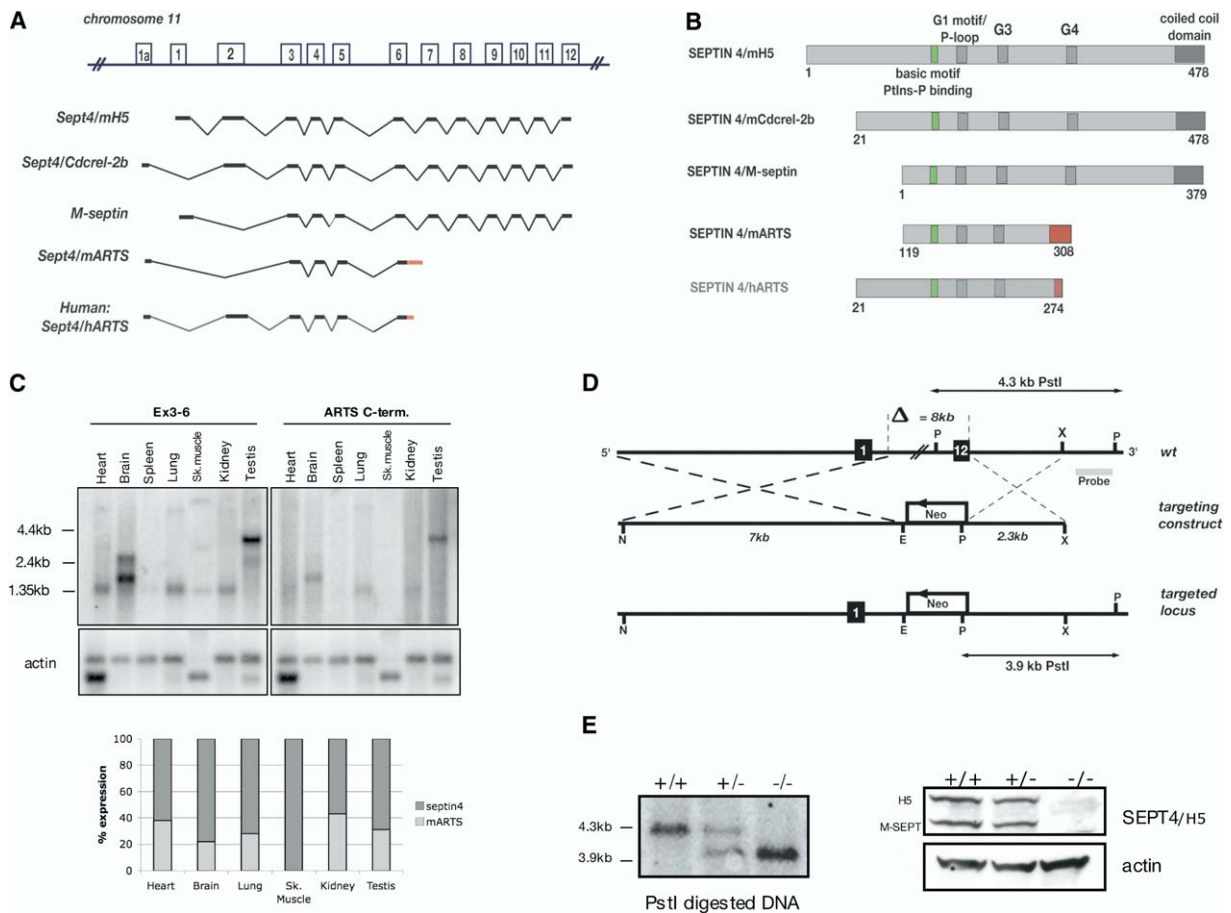
Figure 1. Targeting of the *Sept4* Locus

(A) Schematic presentation of major transcripts derived from the *Sept4* locus. *Sept4/Cdcrel2b*, *Sept4/*mARTS, and *Sept4/*hARTS utilize an upstream ATG start site, shown as exon 1a. The unique C terminus of mouse ARTS is indicated as a gray bar, and the comparison to human ARTS is shown.

(B) Proteins generated at the *Sept4* locus differ in their N and C termini. Protein motifs, including the GTPase domain (G1, G3, G4, gray boxes), the basic motif (green box) mediating phosphatidylinositol binding and protein localization (Casamayor and Snyder, 2003; Zhang et al., 1999), as well as the C-terminal coiled coil domain (dark gray box), are indicated. Variability at the N terminus gives rise to proteins with different properties and subcellular location. Numbers of the starting amino acid referring to full-length SEPT4/H5 protein are shown.

(C) Upper panel: tissue Northern blot showing the expression of *Sept4* transcripts in the mouse by using a probe spanning exons 3–6 and a probe specific for the unique C terminus of ARTS. The large size of the testis transcripts appears to result from the presence of additional untranslated sequences due to the use of a distinct, testis-specific promoter. Notice the presence of multiple transcripts as well as the unique expression profile in testis. RNA loading was assessed by reprobing with β-actin. Lower panel: quantification of ARTS mRNA expression in various tissues compared to the total level of *Sept4* transcripts.

(D) Schematic representation of the targeting strategy showing the wt genomic locus on chromosome 11, targeting vector, and mutant allele. Successful integration of the targeting vector results in deletion of exons 2–12 through insertion of a PGK-neomycin selection cassette. Exons are shown as black boxes. The location of the probe used for genomic Southern blot analysis identifying the correct targeting event is shown. Restriction enzymes are P (PstI), X (XhoI), and E (EcoRI).

(E) Left panel: genomic tail DNA digested with PstI shows the proper insertion of the targeting vector, indicated by the presence of the novel 3.9 kb genomic fragment. Right panel: Western blot analysis with an exon 1 peptide antibody. Extracts from cerebellum confirmed the absence of *Sept4* isoforms H5 and M-Septin in mutant mice.

(Figures 3B and 3C). The *Sept4* null sperm isolated from testis (not shown) or from the caput epididymis did not display the 180° bend in the tail seen in cauda sperm, but a defect was detected at the midpiece-principal piece junction. By light microscopy, a thinning of the tail diameter was seen in this region (Figure 3G, arrow), suggesting a defect during the late stages of spermatogenesis, known as spermiogenesis. Although mutant sperm displayed this structural feature already in the testis, onset of severe bending did not occur until the sperm entered the corpus epididymis (Figure 3H). By the time sperm reached the cauda epididymis, 50%–70% displayed this morphological bending (Figure 3I).

Sperm isolated from heterozygote animals revealed an intermediate phenotype, with many sperm showing an L-shaped morphology (20%–30%) and a failure to straighten during their passage through the epididymis (Figures 3D–3F). However, the fertility of heterozygote
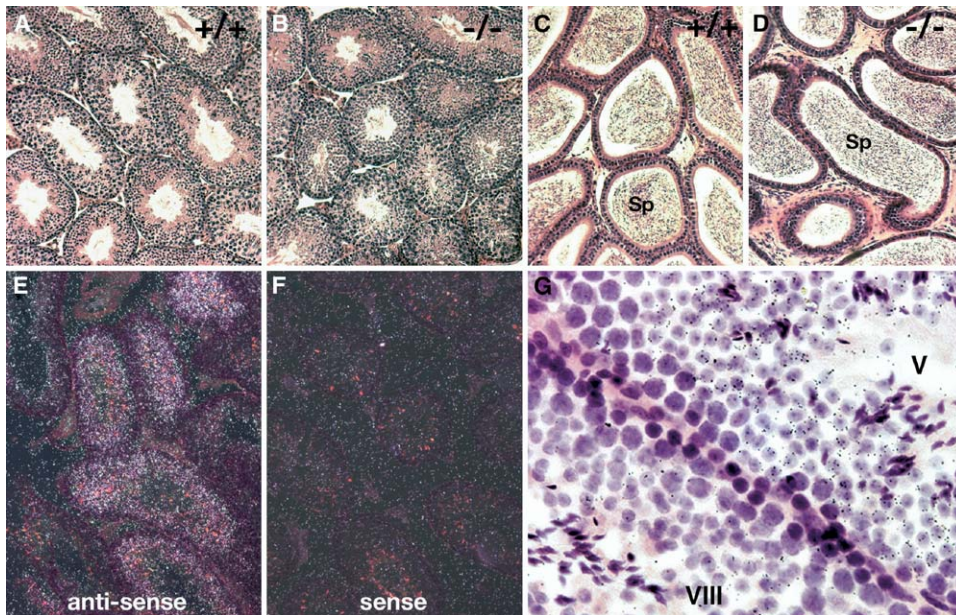
Figure 2. *Sept4* Null Males Are Sterile but Have Overall Normal Testicular Morphology

(A and B) Hematoxylin and eosin staining of paraffin sections showed no difference in the overall morphology of germ cells in (A) wt (10×) and (B) mutant (10×) seminiferous tubules.

(C and D) Loss of *Sept4* function did not block the generation of sperm (sp), as shown by filled tubules of cauda epididymis in (C) wt (10×) and (D) homozygous mutant (10×) males.

(E and F) The expression of *Sept4* transcripts is developmentally regulated and restricted to stage V–VII tubules. RNA in situ hybridization with a GFP-specific probe on testis of *Sept4*-EGFP reporter mice revealed specific staining only in a subset of seminiferous tubules ([E], 10×; [F], control).

(G) Activity of the *Sept4* promoter was specifically detected in postmeiotic cells with the majority of grains localized in round spermatids (stage V tubule, 40×). Note the absence of a specific signal in the adjacent stage VIII tubule, indicating a requirement of *Sept4* proteins in the postmeiotic differentiation of male germ cells.

males was not significantly reduced compared to wt mice. Germ cells remain connected through cytoplasmic bridges throughout spermatogenesis, forming large syncitia and thereby sharing RNAs and proteins. Likely due to this compensation, haploid sperm from heterozygous *Sept4* males carrying the mutant locus were able to be motile and fertile, generating the Mendelian frequencies of genotypes described above. Therefore, loss of *Sept4* function caused male sterility without disturbing testicular and epididymal morphology, while affecting the quality of sperm being produced.

Sept4 Proteins Are Essential in Establishing the Annulus

The bending of mutant sperm suggested a defect in the architecture of the sperm annulus, a ring-like, filamentous structure suggested to form a diffusion barrier between the midpiece and the principal piece of the tail (Cesario and Bartles, 1994; Myles et al., 1984). Interestingly, immunofluorescent staining with an antibody against exon 1 sequences (Takahashi et al., 2003) stained specifically the annulus region of isolated cauda sperm (Figures 4A and 4B), indicating that *Sept4* proteins locate to this structure. Using electron microscopy (EM) on purified sperm from the cauda epididymis, the annulus was easily identified in wt sperm at

the midpiece boundary (Figure 4C, arrow; Figure 4D, bracket) as an hourglass-shaped structure in cross-section, a hallmark of septin ring structures (Moffat and Andrews, 2003). Strikingly, the annulus was completely absent in mutant sperm (Figures 4E and 4F, arrows), and this presumably contributed to the observed bending (Figure 4G). The region immediately following the midpiece-principal piece tail transition was often devoid of the transverse ribs of the fibrous sheath, suggesting an organizational role of the annulus for proper architecture of the tail (Figures 4F and 4G).

Mitochondrial Defects in *Sept4* Mutant Sperm

During spermatogenesis, mitochondria become organized in a highly ordered fashion along the axoneme surrounding the midpiece of the sperm. Our EM analysis of purified cauda sperm showed different densities in the membrane materials of wt and homozygous mutant sperm (Figures 4D, 4F, and 4G). To exclude fixation artifacts on isolated sperm, we performed in situ EM of the cauda epididymis (wt N = 2, ± N = 1, Null N = 3). Mitochondria in wt sperm appeared to be very homogenous in terms of size and distribution of mitochondrial membrane material along the axoneme (Figures 5A, 5B, and 5E). No abnormalities in mitochondrial structure were detected in the heterozygous animal analyzed (not shown). In contrast, mitochondria from *Sept4* mu-

caput **corpus** **cauda**
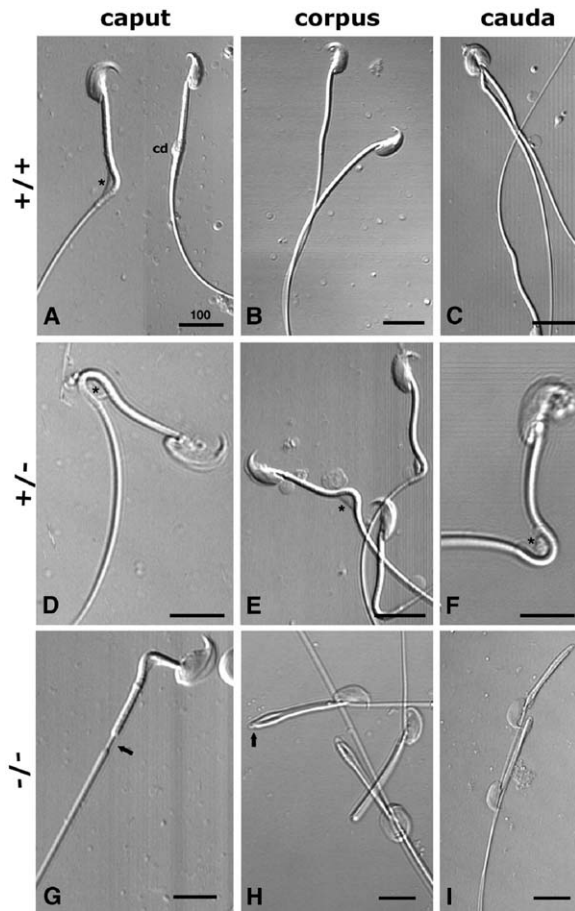
Figure 3. Structural Defects in *Sept4* Null Sperm

(A–I) Brightfield micrographs of purified sperm from caput, corpus, and cauda epididymis representing different stages of maturation. (A) Wt sperm entering the epididymis showed residual cytoplasm (asterisk) and a cytoplasmic droplet (cd). (B and C) Typical straight morphology of wt sperm is seen after further passage through corpus and cauda epididymis. (D–F) An intermediate phenotype in sperm from heterozygous mice resulted often in an L-shaped morphology. Residual cytoplasm is shown attached to maturing sperm (asterisks). (G) *Sept4* null sperm showed structural defects evident as a thinning of the tail region immediately following the sperm midpiece (arrow). (H) The onset of severe bending of mutant sperm occurred during the passage through the corpus epididymis. The arrow in (H) indicates the midpiece-tail boundary. (I) The majority of mutant sperm displayed tail angulations in the cauda epididymis. All images were taken with a 40× lens and were magnified by using LSM confocal software. The scale bar represents 100 μm.

tant sperm contained fewer cristae and hence possessed less membrane material (Figures 5C, 5D, and 5F); thus, they often displayed a single membrane spanning across the mitochondrion (asterisk in Figure 5C). Additionally, in contrast to the highly homogenous size of mitochondria in wt, mitochondria in the *Sept4* null mice varied greatly in size (Figure 5F), disrupting their normally regular and precise arrangement. Frequently, much smaller mitochondria were stacked between their neighbors (Figure 5D, arrows), and some mitochondria appeared to have fission defects (Figure 5D, arrows). These phenotypes were seen in every mu-

tant sperm analyzed, although there was variation amongst individual mitochondria within a sperm. Analyses with mitochondria-selective probes that accumulate in actively respiring mitochondria (MitoTracker Green FM, MitoTracker RedCMXRos) showed no difference in the staining patterns of wt and sperm from *Sept4* null mice, indicating that mutant mitochondria are metabolically active (Figure S3A). To investigate if the observed mitochondrial phenotype is restricted to testis, we performed EM analysis on mitochondria of heart and liver in *Sept4*-deficient mice. Mitochondrial architecture and morphology in these tissues did not differ between *Sept4* null and wt animals (Figure S2). This suggests that mitochondrial *Sept4* proteins are required for mitochondrial integrity in a tissue-specific manner.

Retention of Cytoplasm during Sperm Maturation in *Sept4* Null Males

Another phenotype of *Sept4* mutant sperm was the retention of cytoplasmic droplets at the head and neck region, and their failure to migrate during sperm maturation (Figure 6). Recently, it was shown that effector caspase activity and an apoptosis-like mechanism are required for spermatid individualization in *Drosophila* (Arama et al., 2003). In particular, during terminal differentiation in this system, caspase activity is necessary to remove bulk cytoplasm and thereby contributes to the migration of the waste bag, where excess cytoplasm is collected. A similar removal of excess cytoplasm occurs during mammalian spermiogenesis (Clermont et al., 1993), but a requirement for caspases remains to be demonstrated. Because one of the proteins derived from the *Sept4* locus, ARTS, can promote caspase activity via IAP inhibition (Gottfried et al., 2004), the retention of cytoplasmic droplets in *Sept4* mutant sperm may be due to reduced caspase activity. Whereas EM analysis of cross-sections of wt sperm showed the characteristic structural features of the midpiece and principal piece (Figure 6A), *Sept4* mutant sperm showed a single plasma membrane encasing both the mid- and principal piece of the sperm tail (Figures 6B and 6C, arrows and asterisk in Figure 6C). This can be explained by the presence of excess cytoplasm between the mid- and principal piece, which may also contribute to the bending of sperm. To test if apoptotic proteins are activated during murine spermatogenesis, as in *Drosophila*, we used an antibody that specifically detects activated caspase3 (Di Cunto et al., 2000). Generally, staining with this antibody is restricted to cells that are doomed to undergo apoptosis. However, mature spermatozoa isolated from testis and caput epididymis showed readily detectable active caspase3 staining in ctyoplasmic droplets, demonstrating that an apoptotic effector caspase is indeed activated during mouse spermiogenesis (Figures 6D–6F). Active caspase3 staining was also seen in cyptolasmic droplets of spermatozoa from *Sept4* null males (Figure 6F, arrow). The activity of caspase3 is negatively regulated by IAPs, such as X-linked IAP (XIAP) (Deveraux et al., 1999). Since the proapoptotic ARTS protein can promote apoptosis and caspase activity by antagonizing IAPs, such as XIAP (Gottfried et al., 2004), loss of this
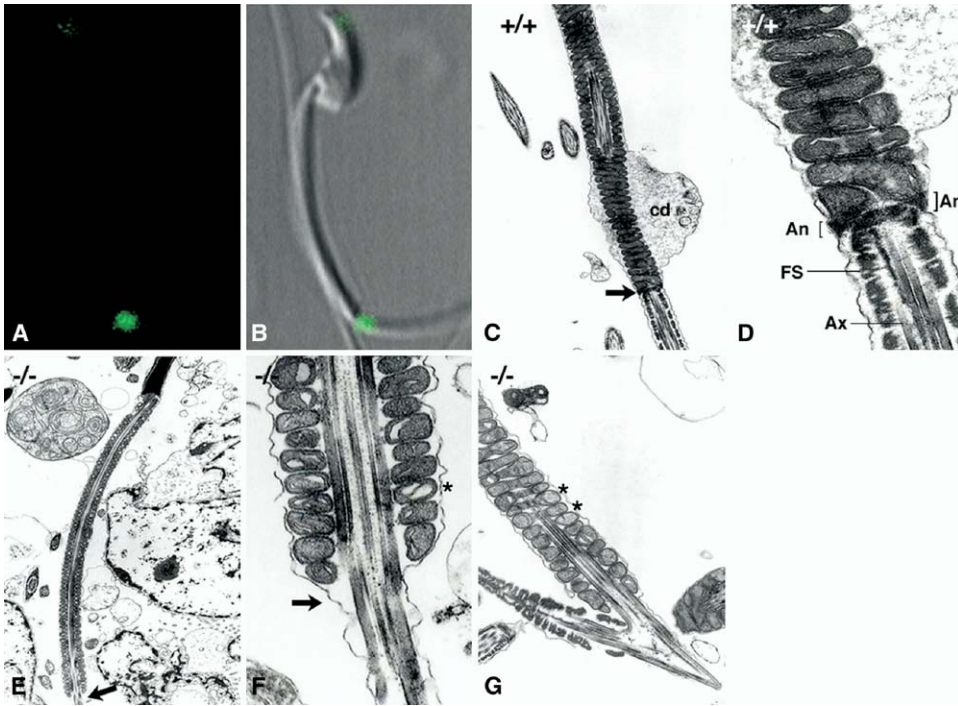
Figure 4. Absence of the Annulus in *Sept4* Null Males

(A and B) Immunostaining of purified epididymal wt sperm from the cauda ([A] FITC channel) with an anti-SEPT4 antibody showed specific staining of the midpiece-tail region ([B] merged FITC brightfield image).

(C) EM analysis of purified sperm from cauda epididymis showed the presence of the annulus in wt sperm (arrow; magnification ×12.500; cd, cytoplasmic droplet).

(D) The annulus was visible as electron-dense filaments displaying an hourglass shape across the sperm plasma membrane (An, annulus; FS, fibrous sheet; Ax, axoneme; magnification ×20.000).

(E and F) The corresponding region in mutant sperm was "empty," with no detectable trace of the annulus (arrows; magnification ×12.500 in [E] and ×20.000 in [F]).

(G) Correlated with this structural deficiency, the principal piece of mutant sperm was severely bent (magnification ×16.500). *Sept4* null sperm also displayed significant mitochondrial defects, including heterogeneity of size and reduced amounts of cristae (indicated by an asterisk in [F] and [G]).

IAP antagonist would be expected to result in reduced caspase3 activity, but not necessarily in reduced caspase3 activation. To further investigate this possibility, we examined the expression of XIAP in spermatids by immunofluorescence staining (Figure 6). Interestingly, XIAP expression was detected in cytoplasmic droplets in a pattern virtually identical to active caspase3 staining (Figure 6G and 6H). In wt cauda sperm, there was only weak staining associated with the cytoplasmic droplet at the annulus (Figure 6G, arrow; Figure S4). However, mutant cauda sperm showed significantly higher intensity of XIAP staining, both in cytoplasmic droplets and in the midpiece region of bent sperm, where we never detected significant XIAP staining in wt (Figures 6H and 6I). Since higher XIAP levels are expected to interfere with caspase3 activity, these observations are consistent with the idea that caspase3 promotes the removal of excess sperm cytoplasm. To further investigate the role of *Sept4* in the removal of residual sperm cytoplasm, we analyzed the localization of cytoplasmic droplets during migration through the epididymis from males of all three genotypes. As shown in Figure 6J, spermatids from homozygous mutant males had residual cytoplasm that remained associated with the neck region and did not migrate toward the annulus after the bulk cytoplasm was removed. Taken together, these findings support the model that *Sept4*/ARTS antagonizes IAPs and thereby derepresses active caspases, which in turn contribute to the removal of cytoplasm during mouse spermiogenesis.

Loss of Capacitation Potential in *Sept4* Mutant Sperm

The potential of sperm to fertilize an oocyte is acquired during its passage through the epididymis (Hunnicutt et al., 1997). We investigated if *Sept4* null sperm underwent the molecular changes in the epididymis necessary for fertility, or if the observed sterility was simply caused by the lack of motility. The fertilization potential of sperm is associated with its capability to sequentially undergo capacitation and the acrosome reaction, two stages of sperm maturation that occur in the female genital tract in preparation for fertilization. During capacitation, sperm become hypermotile, many proteins are phosphorylated, and membrane proteins and lipids rearrange (Hunnicutt et al., 1997; Travis et al., 2001b). Although capacitation occurs within the female, it can be mimicked in vitro (Visconti et al., 1998). We
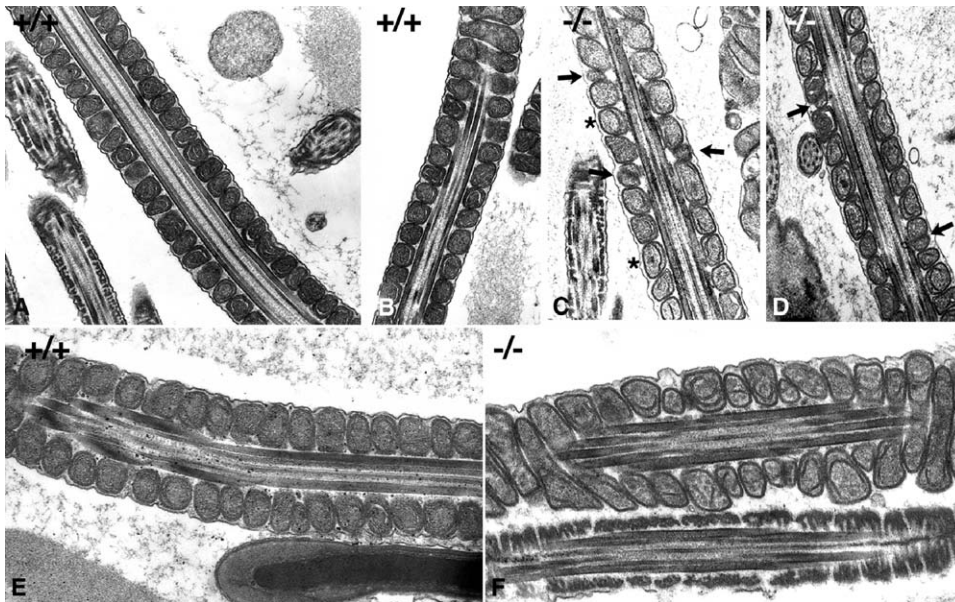
Figure 5. Defects in Mitochondrial Architecture in *Sept4* Null Sperm

(A , B, and E) In situ EM analysis of the cauda epididymis revealed a high degree of homogeneity in the size and arrangements of mitochondria in wt sperm along the axoneme in the midpiece region. (C–F) (C, D, and F) In contrast, mitochondria in *Sept4* null sperm had variable size and irregular appearance, and they often displayed severely reduced membrane material. Sometimes, mitochondria appeared "empty" and almost devoid of any cristae (asterisks in [C]). Note the presence of many abnormally small mitochondria (arrows in [C] and [D]; [F]).

purified wt, heterozygous, and *Sept4* null sperm from cauda epididymis, placed them in capacitating conditions, and immunoblotted the sperm for protein phosphorylation. Mature wt and heterozygous cauda sperm showed the characteristic 96 kd phopshotyrosine band in the uncapacitated state and gain the typical phosphotyrosine profile associated with capacitation (Figure 7). In contrast, even baseline tyrosine phopshorylation in uncapacitated cauda sperm was absent in the mutant, and no additional phopshorylation events were observed after β-cyclodextrin stimulation.

Discussion

To investigate the function of the *Sept4* septin locus in the mouse, we generated a targeted deletion on chromosome 11 eliminating the entire coding region of this locus. Our study shows a strict requirement for *Sept4* during the late stages of spermiogenesis and points toward an evolutionary conserved function of these proteins in this highly specialized tissue in mammals. Some of the *Sept4* mutant phenotypes that we observed can be explained based on the traditional view of septins as filamentous proteins, but our data also support a physiological role of this locus in caspase regulation.

To date, the analysis of septin function in vivo has been complicated by the complex interaction between septin family members in formation of the septin cytoskeleton (Kinoshita, 2003). For instance, analysis of Septin5-deficient mice revealed compensation of Septin5 function through alterations in the expression profiles of other septin genes, resulting in no phenotypic

abnormalities in the tissues analyzed (Peng et al., 2002). In addition, purification and analysis of Septin2 protein complexes from mouse brain identified six other interacting septins, including Septin4, clearly emphasizing the heterogeneity in septin biology (Kinoshita et al., 2002). Compensatory expression of other septin proteins is likely responsible for no gross phenotypic abnormalities in tissues from *Sept4*-deficient mice previously shown to have high *Sept4* expression, like heart and brain. However, our study revealed specific roles of *Sept4* proteins in murine sperm that cannot be compensated for by the function of other septins. First, none of our mutant male mice were able to sire offspring, although their mating behavior, testicular and epididymal morphology, and the number of mature sperm produced were normal. *Sept4* function appears to be specifically required during the postmeiotic stages of terminal sperm differentiation, as indicated by the tightly regulated expression pattern during mouse spermatogenesis, just prior to sperm terminal differentiation. In the absence of *Sept4* proteins, no annulus was formed. The annulus is a ring-like structure composed of filamentous material at the junction between the middle and principal piece of the sperm tail. Although it has been recognized for several decades, its exact nature and biology has remained elusive (Clermont et al., 1993). Based on morphological observations, an active role for the annulus in establishing mitochondrial distribution has been suggested (Phillips, 1977). However, our data indicate that many aspects of spermiogenesis can proceed without the annulus. Mitochondrial migration and overall alignment along the midpiece were not affected, although mitochondria in
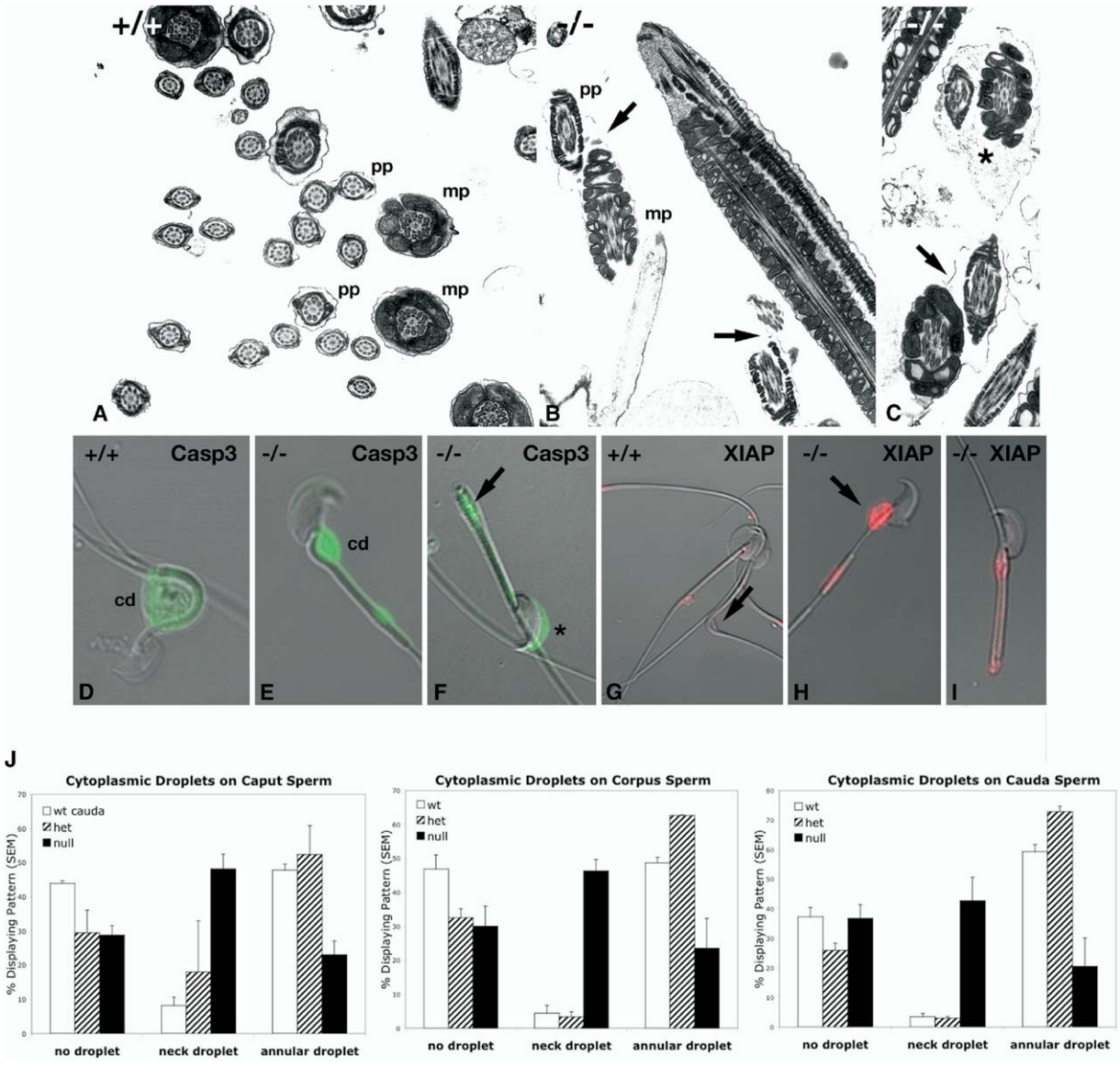
Figure 6. Retention of Residual Cytoplasm in Homozygous Mutant Sperm

(A–C) EM analysis of cross-sections of (A) wt and (B and C) mutant sperm. (A) Cross-sections of the midpiece (mp) and principal piece (pp) showed mitochondria and structural components of the normal sperm tail. (B and C) In *Sept4* null sperm, the midpiece and principal piece of the tail were encased by a single plasma membrane (arrows in [B] and [C]), apparently due to the presence of excess cytoplasm between these parts of the tail (asterisk in [C]).

(D–F) Immunofluorescence staining with an antibody against cleaved caspase3-labeled cytoplasmic droplets (cd; [D] and [E]) in developing mouse sperm, indicating that the apoptotic effector caspase is activated during mammalian spermiogenesis. Cleaved caspase3 staining was seen in both (D) wt and (E and F) homozygous mutant sperm. The arrow in (F) points to residual, activated caspase3-postive cytoplasm at the tail bend. (F) Occasional staining of the acrosome with anti-activated caspase3 antibodies was observed in sperm from the corpus epididymis (asterisk).

(G–I) Immunofluorescence staining revealed that the caspase inhibitor XIAP is present in cytoplasmic droplets in sperm from the cauda epididymis. (G) In wt sperm, anti-XIAP staining was weak and restricted to the annulus region (arrow). In *Sept4* null sperm, anti-XIAP staining was more intense in (H) retained cytoplasm (arrow) and can also be detected throughout the (I) midpiece region.

(J) Quantitative representation of cytoplasmic defects in *Sept4* null sperm. Sperm was isolated from different regions of the epididymis (caput, corpus, cauda) from males of all genotypes (wt N = 5, heterozygous N = 6, *Sept4* null N = 7), and the localization of residual cytoplasm was evaluated by phase contrast microscopy. Residual cytoplasm in *Sept4* null sperm was being retained at the head and neck region of sperm throughout the epididymis. Results are expressed as the mean and standard deviation from the indicated number of mice (see the Experimental Procedures).
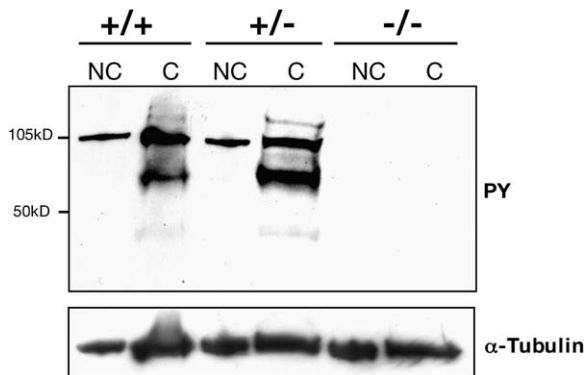
Figure 7. *Sept4* Null Sperm Are Capacitation Defective

Phosphorylation profiles of purified sperm from cauda epididymis before and after capacitation stimulated by the addition of β-cylco-dextrin. The absence of even basal levels of phosphorylation was observed in mutant sperm. Shown are Western blots of different genotypes from cauda sperm using an anti-phosphotyrosine-specific antibody.

Sept4 null animals were of more heterogeneous size than in wt (see below). The main defect associated with the lack of the annulus was a severe bending of the sperm tail.

There are several additional distinct structural defects that are likely to contribute to male infertility. For one, *Sept4* mutant sperm do not develop the ability to swim, a function that is acquired during passage through the epididymis, indicating that mutant sperm is not undergoing molecular changes for proper maturation. To investigate if other epididymal functions are lost, we investigated the capacitative ability of mutant sperm during epididymal transit. The molecular events regulating this process were shown to result in a characteristic phosphorylation profile generated in a protein kinase A-dependent manner, yet the exact biochemical pathway remains poorly understood (Visconti et al., 1995). *Sept4* mutant sperm are unable to acquire these characteristic changes during epididymal transit, as even basal levels of tyrosine phosphorylation are absent, indicating that upstream signaling events, which confer sperm maturation, are not activated. Sperm are highly compartmentalized, and the distribution of some proteins changes from the principal piece of the tail to a diffuse pattern throughout the sperm during the capacitation process (Cesario and Bartles, 1994; Myles and Primakoff, 1984). The annulus was proposed to regulate this process at the midpiece-principal piece junction by establishing a diffusion barrier, similar to the ascribed function of the septin ring in maintaining cell polarity during mitotic division in *Saccharomyces cerevisiae* (Longtine and Bi, 2003). An exact function for redistribution of proteins during capacitation is not known. However, the absence of the annulus in *Sept4* null males might interfere with the proper localization of proteins during capacitation, leading to free diffusion and thereby preventing the initiation of the tyrosine phosphporylation cascade.

Sept4 mutant sperm also displayed structural de-

fects that are consistent with abnormal mitochondrial fission. Mitochondria are highly dynamic organelles that undergo fission and fusion depending on the developmental and physiological state of the cell (Karbowski and Youle, 2003; Yaffe, 1999). During spermiogenesis, mitochondria undergo a dramatic reorganization in the midpiece of the sperm tail, resulting in a helical alignment of similarly shaped and sized organelles along the cytoskeletal components of the sperm axis, referred to as the mitochondrial sheath. In contrast to the homogenous, regular appearance of mitochondria in wt, mitochondria in *Sept4* null sperm appeared disorganized and heterogeneous in size, and they had reduced amounts of cristae.

These defects could stem from partially defective fission or fusion events that take place prior to mitochondrial reorganization. Given the role of cytoplasmic septins in cytokinesis, it is attractive to speculate that mitochondrial septins, like SEPT4/M-septin or ARTS, may be involved in mitochondrial fission. However, direct experimental evidence for such a role remains to be established.

Another striking phenotype of *Sept4* mutant mice was the retention of cytoplasmic droplets at the head and neck region of mutant sperm. During mammalian spermiogenesis, round spermatids elongate and differentiate into mature spermatozoa. At the late stages during this differentiation process, the bulk of cytoplasm of elongating spermatids is moving toward the head and neck region and is being shed, leaving behind residual cytoplasm referred to as the cytoplasmic droplet (Clermont et al., 1993). Retention of excess cytoplasm has been associated with a variety of human infertility syndromes (Cooper, 2005). During migration of sperm through the mouse epididymis, the cytoplasmic droplet typically moves toward the annulus region (Cooper and Yeung, 2003). In *Drosophila*, elimination of the bulk cytoplasm during late spermiogenesis involves an apoptosis-like mechanism and requires caspase activity (Arama et al., 2003). Intriguingly, the retention of cytoplasm in sperm from *Sept4* mutant males is overall similar to defects seen upon inhibiting caspase activity in *Drosophila* sperm. Like in *Drosophila*, caspase3, an apoptotic effector caspase, is activated in postmeiotic germ cells. Generally, active caspase3 is only detected in cells that are destined to undergo apoptosis. Therefore, it is tempting to speculate that, analogous to the situation in *Drosophila*, this apoptotic effector caspase contributes to the removal of bulk cytoplasm, and that the retention of cytoplasm results from insufficient caspase activity. Significantly, one of the proteins derived from the *Sept4* locus, ARTS, was previously shown to promote caspase activity through IAP inhibition, whereas other *Sept4* protein isoforms did neither bind to IAPs nor promote caspase activation and apoptosis (Larisch et al., 2000, Gottfried et al., 2004). Furthermore, ARTS can promote the degradation of XIAP by ubiquitin-mediated protein degradation (Gottfried et al., 2004). Since IAPs can directly inhibit active caspase3 (Deveraux et al., 1999), loss of an IAP antagonist, such as ARTS, is expected to increase XIAP activity and hence reduce the activity of caspase3, but not necessarily the conversion of pro-casapase3 to active cas-

pase3. Consistent with this model, we observed increased immunostaining of the XIAP caspase inhibitor protein, but no overt differences in caspase3 activation in mutant sperm. These observations suggest that the apoptotic machinery may contribute to differentiation of mammalian sperm by promoting the removal of residual cytoplasm.

Taken together, our results indicate that *Sept4* proteins are likely to act at multiple stages during late sperm differentiation by influencing mitochondrial morphology, establishing the annulus, and regulating of cytoplasmic dynamics. The described features of the annulus as a ring-like cytoskeletal structure and diffusion barrier to establish cellular compartmentalization are strikingly similar to the function of the septin ring in *Saccharomyces cerevisiae* during cytokinesis and suggest evolutionary conservation of septin function between yeast and mammals. The finding that mutations in *Sept4* proteins can lead to male sterility without affecting testicular function or morphology underscores the importance of the as yet unknown molecular machinery during epididymal transit that generates functional gametes and motile sperm. Dissecting the contribution of individual *Sept4* variants during the sperm maturation process may provide new drug targets for the development of male contraceptives. Furthermore, understanding the contribution of the apoptotic machinery in this process may also provide insights into the cause of droplet sperm, a major human male infertility syndrome.

Experimental Procedures

Cloning of the Targeting Vector and Generation of Mutant Mice
A genomic fragment carrying the entire mouse *Sept4* locus was isolated by screening a genomic BAC library (Invitrogen, clones 96022) from CJ7 ES cells derived from 129S1/Sv mice (stock 00090) with a ^{32}P-labeled PCR probe derived from exon 2 of Septin4/H5. A replacement targeting vector was constructed (Figure 1D), with correct targeting resulting in deletion of 8 kb of the genomic *Sept4* locus. Recombinant ES cell clones were identified by Southern blot analysis and injected into C57BL/6J blastocysts. One of the injected clones successfully contributed to the mouse germline and gave rise to hemizygous animals. F1 mice were then intercrossed to generate *Sept4* null mice (C57BL/6J;129Sv).

Northern Blot Analysis, RT-PCR, and Western Blot Analysis
A multiple tissue Northern blot (MTN, BD Biosciences Clontech) was hybridized with a ^{32}P-labeled probe spanning Ex3–Ex6 and detecting all *Sept4* transcripts (Figure 1) or a probe specific for the ARTS unique C terminus that was generated by PCR from an EST (forward primer: 5′-GCCACGGGTATGGTC-TGAGCC-3′, reverse primer: 5′-TCAACATCCAATGGCCGGAGC-3′). The absence of *Sept4* transcripts of all sizes was confirmed by Northern blot analysis with testis and brain RNA of *Sept4* null mice. ARTS expression was quantified by using a phosphoimager and IMAGE Quant software. RT-PCR was performed by using the ONE-Step RT-PCR kit from InVitrogen on RNA prepared from testis and brain. Protein from mice of all genotypes was extracted from cerebellum, separated by SDS-PAGE, and transferred to nitrocellulose for blot analysis with anti-SEPT4 antibody (1:2000).

RNA In Situ Hybridization
Sept4-EGFP transgenic mice were obtained from the GENSAT project at Rockefeller University (Gong et al., 2003). Detailed information about the generation of the *Sept4* BAC transgenic line can be obtained at www.gensat.org (Heintz and Hatten, 2004) Single-stranded, ^{33}P-labeled GFP RNA probes were prepared from linear-ized plasmids with T7 or Sp6 RNA polymerases by using a ribonucleotide triphosphate mix containing 12 μM cold UTP and 4 μM hot UTP. Corresponding sense RNA served as a negative control. The RNA in situ hybridization procedure was essentially carried out as described previously (Manova et al., 1990). Slides were developed after 14 days of exposure.

Histological Analysis and Sperm Preparation
Testis and epididymis were dissected and fixed in Bouin's fixative or 4% paraformaldehyde at 4°C overnight. The tissues were dehydrated in ethanol, embedded in paraffin, sectioned at 10 μm, and stained in Gill's hematoxylin and eosin staining. For analysis of mature spermatozoa, testis, caput, corpus, and cauda epididymis were dissected and placed in noncapacitating medium (22 mM HEPES, 1.2 mM MgCl$_2$, 100 mM NaCl, 4.7 mM KCl, 1.0 mM pyruvic acid, 5.5 mM glucose, 4.8 mM lactic acid [pH 7.3]) (Travis et al., 2001a). Tissues were diced to allow sperm to seep out and filtered through a 100 μm mesh for analysis.

Ultrastructural Studies
Cauda epididymis was dissected, and the tissue was fixed in 2.5% glutaraldehyde/100 mM cacodylic buffer (pH 7.4) for in situ analysis. Sperm were prepared as described and fixed in suspension. Tissue or cells were postfixed in 1% osmium tetroxide, dehydrated, and processed for routine transmission electron microscopy. Characterization of mitochondrial phenotypes was performed through double blind analysis, and only mitochondria at the plane of the axoneme were compared.

Immunofluorescence Staining
Sperm suspensions were fixed in 3% paraformaldehyde and permeabilized by consecutive freeze-thaw cycles or 10 min of treatment with 0.5% Triton-X. Cells were blocked in 0.2% gelatin, 0.5% BSA in PBS (PBG) and incubated with antibody dilutions at 4°C overnight. *Sept4*/H5 antibody was a generous gift from S. Yanagi (1:50). Anti-active caspase3 (BD PharMingen CM1, 1:1000; Figure 6), cleaved capase3 antibody (Cell Signaling 9661B, 1:50), and anti-XIAP (RD Systems, clone MAB822; Sigma X2505, both 1:20) were also used. As a negative control, β-GAL antibody from the same species as the experimental antibody was used. Images of control and homozygous mutant mice were taken with a Zeiss LSM500 confocal microscope at the same instrument settings.

Capacitation Reaction
Sperm suspensions from cauda epididymis were suspended at 6.5×10^6 cells in noncapacitating medium and capacitated at 37°C for 60 min by addition of 2 mM β-cyclodextrin. Sperm were then washed in capacitating medium containing 0.2 mM Na$_3$VO. 1.3×106 cells/lane were subjected to SDS-PAGE and were transferred to nitrocellulose for anti-phosphotyrosine blot analysis (Upstate, 4G10, 1:1000).

Supplemental Data
Supplemental Data include further information on the expression of an ARTS-like splice variant in testis and addresses in more detail the specific localization of *Sept4* transcripts during spermiogenesis. Evidence is provided that the observed mitochondrial defects are tissue specific. Further examples of wt and *Sept4* null sperm underscore the effect of the mutation on the regulation of XIAP levels in sperm carrying the mutant allele, as indicated by the enhanced staining in the sperm midpiece. Supplemental Data are available at http://www.developmentalcell.com/cgi/content/full/8/3/353/DC1/.

References

Arama, E., Agapite, J., and Steller, H. (2003). Caspase activity and a specific cytochrome C are required for sperm differentiation in *Drosophila*. Dev. Cell *4*, 687–697.

Barral, Y., Mermall, V., Mooseker, M.S., and Snyder, M. (2000). Compartmentalization of the cell cortex by septins is required for maintenance of cell polarity in yeast. Mol. Cell *5*, 841–851.

Casamayor, A., and Snyder, M. (2003). Molecular dissection of a yeast septin: distinct domains are required for septin interaction, localization, and function. Mol. Cell. Biol. *23*, 2762–2777.

Castillon, G.A., Adames, N.R., Rosello, C.H., Seidel, H.S., Longtine, M.S., Cooper, J.A., and Heil-Chapdelaine, R.A. (2003). Septins have a dual role in controlling mitotic exit in budding yeast. Curr. Biol. *13*, 654–658.

Cesario, M.M., and Bartles, J.R. (1994). Compartmentalization, processing and redistribution of the plasma membrane protein CE9 on rodent spermatozoa. Relationship of the annulus to domain boundaries in the plasma membrane of the tail. J. Cell Sci. *107*, 561–570.

Clermont, Y., Oko, R., and Hermo, L. (1993). Cell biology of mammalian spermiogenesis. In Cell and Molecular Biology of the Testis, C. Desjardins and L.L. Ewing, eds. (New York: Oxford University Press), pp. 332–376.

Cooper, T.G. (2005). Cytoplasmic droplets: the good, the bad or just confusing? Hum. Reprod. *20*, 9–11.

Cooper, T.G., and Yeung, C.H. (2003). Acquisition of volume regulatory response of sperm upon maturation in the epididymis and the role of the cytoplasmic droplet. Microsc. Res. Tech. *61*, 28–38.

Deveraux, Q.L., Stennicke, H.R., Salvesen, G.S., and Reed, J.C. (1999). Endogenous inhibitors of caspases. J. Clin. Immunol. *19*, 388–398.

Di Cunto, F., Imarisio, S., Hirsch, E., Broccoli, V., Bulfone, A., Migheli, A., Atzori, C., Turco, E., Triolo, R., Dotto, G.P., et al. (2000). Defective neurogenesis in citron kinase knockout mice by altered cytokinesis and massive apoptosis. Neuron *28*, 115–127.

Dobbelaere, J., Gentry, M.S., Hallberg, R.L., and Barral, Y. (2003). Phosphorylation-dependent regulation of septin dynamics during the cell cycle. Dev. Cell *4*, 345–357.

Elhasid, R., Sahar, D., Merling, A., Zivony, Y., Rotem, A., Ben-Arush, M., Izraeli, S., Bercovich, D., and Larisch, S. (2004). Mitochondrial pro-apoptotic ARTS protein is lost in the majority of acute lymphoblastic leukemia patients. Oncogene. *23*, 9450.

Faty, M., Fink, M., and Barral, Y. (2002). Septins: a ring to part mother and daughter. Curr. Genet. *41*, 123–131.

Field, C.M., Coughlin, M.L., Straight, A.F., and Mitchison, T.J. (2002). Septins: cytoskeletal polymers or signalling GTPases? Dev. Cell *3*, 791–802.

Gong, S., Zheng, C., Doughty, M.L., Losos, K., Didkovsky, N., Schambra, U.B., Nowak, N.J., Joyner, A., Leblanc, G., Hatten, M.E., and Heintz, N. (2003). A gene expression atlas of the central nervous system based on bacterial artificial chromosomes. Nature *425*, 917–925.

Gottfried, Y., Rotem, A., Lotan, R., Steller, H., and Larisch, S. (2004). The mitochondrial ARTS protein promotes apoptosis through targeting XIAP. EMBO J. *23*, 1627–1635.

Hartwell, L.H. (1971). Genetic control of the cell division cycle in yeast. IV. Genes controlling bud emergence and cytokinesis. Exp. Cell Res. *69*, 265–276.

Heintz, N., and Hatten, M.B. (2004). The Gene Expression Nervous System Atlas (GENSAT) Project (www.gensat.org).

Hunnicutt, G.R., Koppel, D.E., and Myles, D.G. (1997). Analysis of the process of localization of fertilin to the sperm posterior head plasma membrane domain during sperm maturation in the epididymis. Dev. Biol. *191*, 146–159.

Karbowski, M., and Youle, R.J. (2003). Dynamics of mitochondrial morphology in healthy cells and during apoptosis. Cell Death Differ. *10*, 870–880.

Kartmann, B., and Roth, D. (2001). Novel roles for mammalian septins: from vesicle trafficking to oncogenesis. J. Cell Sci. *114*, 839–844.

Kim, D.S., Hubbard, S.L., Peraud, A., Salhia, B., Sakai, K., and Rutka, J.T. (2004). Analysis of mammalian septin expression in human malignant brain tumors. Neoplasia *6*, 168–178.

Kinoshita, M. (2003). Assembly of mammalian septins. J. Biochem. (Tokyo) *134*, 491–496.

Kinoshita, M., Field, C.M., Coughlin, M.L., Straight, A.F., and Mitchison, T.J. (2002). Self- and actin-templated assembly of mammalian septins. Dev. Cell *3*, 791–802.

Larisch, S., Yi, Y., Lotan, R., Kerner, H., Eimerl, S., Tony Parks, W., Gottfried, Y., Birkey Reffey, S., de Caestecker, M.P., Danielpour, D., et al. (2000). A novel mitochondrial septin-like protein, ARTS, mediates apoptosis dependent on its P-loop motif. Nat. Cell Biol. *2*, 915–921.

Larisch-Bloch, S., Danielpour, D., Roche, N.S., Lotan, R., Hsing, A.Y., Kerner, H., Hajouj, T., Lechleider, R.J., and Roberts, A.B. (2000). Selective loss of the transforming growth factor-beta apoptotic signaling pathway in mutant NRP-154 rat prostatic epithelial cells. Cell Growth Differ. *11*, 1–10.

Longtine, M.S., and Bi, E. (2003). Regulation of septin organization and function in yeast. Trends Cell Biol. *13*, 403–409.

Manova, K., Nocka, K., Besmer, P., and Bachvarova, R.F. (1990). Gonadal expression of c-kit encoded at the W locus of the mouse. Development *110*, 1057–1069.

Moffat, J., and Andrews, B. (2003). Ac'septin' a signal: kinase regulation by septins. Dev. Cell *5*, 528–530.

Myles, D.G., and Primakoff, P. (1984). Localized surface antigens of guinea pig sperm migrate to new regions prior to fertilization. J. Cell Biol. *99*, 1634–1641.

Myles, D.G., Primakoff, P., and Koppel, D.E. (1984). A localized surface protein of guinea pig sperm exhibits free diffusion in its domain. J. Cell Biol. *98*, 1905–1909.

Peng, X.R., Jia, Z., Zhang, Y., Ware, J., and Trimble, W.S. (2002). The septin CDCrel-1 is dispensable for normal development and neurotransmitter release. Mol. Cell. Biol. *22*, 378–387.

Phillips, D.M. (1977). Mitochondrial disposition in mammalian spermatozoa. J. Ultrastruct. Res. *2*, 144–154.

Salvesen, G.S., and Abrams, J.M. (2004). Caspase activation — stepping on the gas or releasing the brakes? Lessons from humans and flies. Oncogene *23*, 2774–2784.

Sassone-Corsi, P. (2002). Unique chromatin remodeling and transcriptional regulation in spermatogenesis. Science *296*, 2176–2178.

Surka, M.C., Tsang, C.W., and Trimble, W.S. (2002). The mammalian septin MSF localizes with microtubules and is required for completion of cytokinesis. Mol. Biol. Cell *13*, 3532–3545.

Takahashi, S., Inatome, R., Yamamura, H., and Yanagi, S. (2003). Isolation and expression of a novel mitochondrial septin that interacts with CRMP/CRAM in the developing neurones. Genes Cells *8*, 81–93.

Takizawa, P.A., DeRisi, J.L., Wilhelm, J.E., and Vale, R.D. (2000). Plasma membrane compartmentalization in yeast by messenger RNA transport and a septin diffusion barrier. Science *290*, 341–344.

Travis, A.J., Jorgez, C.J., Merdiushev, T., Jones, B.H., Dess, D.M., Diaz-Cueto, L., Storey, B.T., Kopf, G.S., and Moss, S.B. (2001a).

Functional relationships between capacitation-dependent cell signaling and compartmentalized metabolic pathways in murine spermatozoa. J. Biol. Chem. *276*, 7630–7636.

Travis, A.J., Merdiushev, T., Vargas, L.A., Jones, B.H., Purdon, M.A., Nipper, R.W., Galatioto, J., Moss, S.B., Hunnicutt, G.R., and Kopf, G.S. (2001b). Expression and localization of caveolin-1, and the presence of membrane rafts, in mouse and Guinea pig spermatozoa. Dev. Biol. *240*, 599–610.

Visconti, P.E., Moore, G.D., Bailey, J.L., Leclerc, P., Connors, S.A., Pan, D., Olds-Clarke, P., and Kopf, G.S. (1995). Capacitation of mouse spermatozoa. II. Protein tyrosine phosphorylation and capacitation are regulated by a cAMP-dependent pathway. Development *121*, 1139–1150.

Visconti, P.E., Galantino-Homer, H., Moore, G.D., Bailey, J.L., Ning, X., Fornes, M., and Kopf, G.S. (1998). The molecular basis of sperm capacitation. J. Androl. *19*, 242–248.

Yaffe, M.P. (1999). The machinery of mitochondrial inheritance and behavior. Science *283*, 1493–1497.

Zhang, J., Kong, C., Xie, H., McPherson, P.S., Grinstein, S., and Trimble, W.S. (1999). Phosphatidylinositol polyphosphate binding to the mammalian septin H5 is modulated by GTP. Curr. Biol. *9*, 1458–1467.